Enhanced Long-run Incremental Cost Pricing Considering the Impact of Network Contingencies

Chenghong Gu, *Student Member, IEEE*, and Furong Li, *Senior Member, IEEE*

***Abstract*—This paper improves the existing Long-run incremental cost (LRIC) pricing which forms the basis for one of the two common charging methodologies that are to be adopted by the UK's 7 distribution network operators for charging customers connected at Extra-high Voltage (EHV) distribution networks from April 2012. . The original model is expected to respect network security while evaluating charges based on the extent of the use of the network, which it achieves by reshaping components' capacity with their contingency factors into maximum available capacity. It then identifies the impact of a nodal injection on each component under normal conditions within the threshold of the maximum available capacity. The problem with the LRIC is that it assumes that the impact from a nodal injection is the same under both normal and contingent states, thus under-estimating its impact under contingencies.**

In this paper, the original LRIC model is improved by considering the respective impacts from users under both normal and contingent conditions. The improved model runs incremental contingency flow analysis to determine how they affect components' flows under contingencies. In order to illustrate the differences in the reinforcement horizons, a comparison of the original and enhanced approaches is carried out on three basic distribution networks: single-branch, parallel-branch, and meshed. The new approach chooses the smaller horizons between those from normal and contingent situations to derive charges. Sensitivity analysis is introduced to reduce the calculation burden in determining components' flow increments due to injections. The improved approach is finally testified and compared with the original model on a three-busbar system and a practical system.

***Index Terms*-- Network pricing, long-run increment cost, security, network contingency.**

I. Introduction

MARKET forces have been playing a vital role in enhancing the efficiency of network operation and planning since privatization and deregulation was introduced into electricity industry worldwide. In this new environment, the relationship between generation, network utility, and demand is commercial. Network utilities provide their networks to generators and loads to transfer their energy supply/demand. Generators and loads thereby should pay for their use of the networks to transport power to points of consumption, which takes the form of use-of-system (UoS) charge, appearing both at transmission and distribution levels [1-5]. Network charging is used to serve the purpose of charging customers according to their use of system.

Long-run pricing methodology entails evaluating investment cost necessary to accommodate new generation and demand in the network and appropriately assigns the cost to network users [1, 6]. Developing an long-run pricing model has been viewed as a formidable task [7-9]. To evaluate future network investment, most existing approaches require a least-cost future network planning against a set of projected generation/load growth patterns, but such evaluation would be very difficult [10] and impractical against every single node of a network. The drawbacks of the approaches are prominent: i) passive, reacting to a set of projected patterns of future generation and demand, thus unable to proactively influence the patterns of future generation/demand through incentives; ii) requiring the knowledge of future generation/demand, which is far from certain and of out operators' control in a competitive environment [11]. Pre 2005, the most advanced incremental cost pricing model is Incremental Cost-Related Pricing (ICRP) devised by National Grid (UK), as it directly links the cost of network reinforcement with nodal generation/demand injections without the least network planning. It has been implemented on Brazilian and the UK's transmission networks, but its disadvantages impede its utilization in distribution systems: i) assuming that the present network is fully utilized and any increment in power flow as a nodal injection requires imminent network reinforcement; ii) assuming that a circuit is infinitely divisible and a unit demand increase can be accommodated by a unit of capacity increase.

In the UK, the watchdog of the UK's electricity and gas markets - the Office of Gas and Electricity Markets (Ofgem) favours two long-run pricing models as common distribution charging methodologies for Extra-high Voltage (EHV) distribution network pricing - Long-run Incremental Cost (LRIC) Pricing and Forward Cost Pricing (FCP). The core of LRIC model was developed by University of Bath (UoB) in conjunction with Ofgem and Western Power Distribution (WPD) [11, 12]. The model is to reflect the impact on future network investment as a result of a tiny connectee at each study node. The core of FCP model was developed by Scottish

The authors are with the Department of Electronic and Electrical Engineering, University of Bath, Bath BA2 7AY, U.K. (e-mail: c.gu@bath.ac.uk; f.li@bath.ac.uk).

and Southern (SSE), Central Networks (CN), and Scottish Power (SP) [13, 14]. The FCP pricing is an average pricing model; it evaluates the total network investment cost over next 10 years and allocates the cost to all existing and forecasted future demand and generation customers. The aim is that the total revenue recovered over the 10 year period equals to the forecasted reinforcement cost over the same period [15]. The two approaches are considered by the industry and Ofgem as the best available approaches to achieve the high level charging principles: cost-reflectivity, simplicity, and predictability. Ofgem allows the 7 Distribution Network Operators (DNOs) in the UK to choose one of the two charging methodologies to implement by April 2012 [16].

The two approaches are able to reflect network security mandated by network security standard in determining customers' influence on future network investment [12, 17]. They respect it by running N-1 or higher level contingencies to identify components' maximum contingency flow. (The definitions of "most serious contingency", "maximum contingency flow", "contingency factor", and "maximum available capacity" are given in the Appendix). Because the LRIC treats demand and generation pricing together rather than separately and produces stronger locational signals over the FCP, our study is aimed at improving the LRIC model.

The LRIC model identifies components' ability to cater for network contingencies by reshaping their rated capacities with their contingency factors to produce their maximum available capacity, where contingency factors are defined as their maximum contingency flows under all contingency events divided by their normal case flows. The flows these components can accommodate can only increase under the threshold of their maximum available capacity. The model then determines how a nodal injection can defer or accelerate components' reinforcement horizons under normal conditions. For simplicity, the original LRIC model assumes that the impacts on components' power flows from a nodal injection are the same under the normal and contingent conditions, and thus it may under or over estimate the injections' impact to the system under contingencies. The generated charges from the model, consequently, therefore, do not fully reflect the extent of the use of the system by customers.

This paper seeks to improve the original LRIC pricing model in [11, 12] to overcome its disadvantage in treating users' impact under contingencies. This proposed model examines the impact from a nodal injection not only under normal conditions but also contingencies. Between the reinforcement horizons of a particular component under the two conditions, the minimum is the time to reinforce the component. In order to demonstrate the concept, the impact of a nodal injection on an asset's investment horizon under contingencies for three radial and meshed networks is studied and compared with the original horizon. For large-scale systems, the proposed concept to examine the impact from an injection at each studied node under both conditions could be time-consuming and thus, sensitivity analysis for both normal and contingent case incremental flow calculations is introduced to save computational effort. The enhanced approach is compared and contrasted with the original model reported in [11, 12] on one three-busbar system and a practical system to demonstrate their difference in terms of asset reinforcement horizons and the consequential charges.

The rest of the paper is organized as follows: in Section II, components' reinforcement horizons calculated under normal conditions are studied. Section III introduces the approach to evaluate their horizons under contingencies. Section IV compares the horizons from the two conditions on three distribution networks. The improved charging framework is proposed in Section V, which is then illustrated and compared with the original model on a simple and a practical distribution networks in Sections VI and VII respectively. Section VIII concludes the paper.

II. Reinforcement Horizons in Normal Conditions

This section determines components' reinforcement horizons with and without injections under normal conditions, demonstrating on a simple system given in Fig. 1.

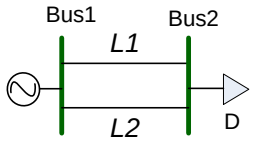

Fig.1. Two-busbar radial system framework.

A. Original Reinforcement Horizons without Injections

The two circuits are assumed to be identical, together supporting a load of D. In order to cater for the maximum additional flow that appears when the other circuit fails, part of each circuit's capacity needs to be reserved, which produces the maximum available capacity, defined as the circuit's rating over its contingency factor. Their reinforcement horizons thus are identified by examining the time taking the flow to grow from current loading level to their maximum available capacities:

$$C = \frac{RC}{CF} = D_l \cdot (1+r)^n \tag{1}$$

where, RC is their rated capacity, CF is their contingency factor, C is their maximum available capacity and D_l is their current loading level, which is half of D if loss is ignored.

Rearranging and taking logarithm of (1) gives,

$$n = \frac{\log\left(RC/CF\right) - \log(D_l)}{\log(1+r)} = \frac{\log C - \log D_l}{\log(1+r)} = \frac{\log\left(C/D_l\right)}{\log(1+r)} \tag{2}$$

B. New Reinforcement Horizon with Nodal Injections

A new nodal increment coming to busbar 2 will change the reinforcement horizons of the two circuits, which can be obtained by replacing $\log D_l$ in (2) with $\log(D_l + \Delta P)$

$$n_{new} = \frac{\log C - \log(D_l + \Delta P)}{\log(1+r)} \tag{3}$$

where, ΔP is the normal flow change along each of the circuits due to the increment.

III. Reinforcement Horizons under Contingencies

This section presents the methodology to evaluate the impact of a nodal injection on components' reinforcement under contingencies.

A. Original Reinforcement Horizon without Injections

For a simple system in Fig.1, the investment horizon of either circuit in the case that the other fails is determined with

$$n_{cont} = \frac{\log RC - \log D_{cont}}{\log(1+r)} \tag{4}$$

where, D_{cont} is the maximum contingency flow along the working circuit.

Rearranging (4) gives

$$n_{cont} = \frac{\log\left(RC \big/ D_{cont}\right)}{\log(1+r)} = \frac{\log\left(\dfrac{RC}{CF} \Big/ \dfrac{D_{cont}}{CF}\right)}{\log(1+r)} = \frac{\log\left(C \big/ D_l\right)}{\log(1+r)} \tag{5}$$

It can be seen that (5) is the same as (2), indicating that in the cases without injections normal and contingent conditions drive component reinforcement in the same way.

B. New Reinforcement Horizon with Nodal Injections

An injection at busbar 2 will generate an incremental contingency flow along the working circuit when the other circuit fails, supposed to be ΔP_{cont}. Under such condition, the two circuits' new reinforcement horizons are changed to

$$n_{cont,new} = \frac{\log RC - \log\left(D_{cont} + \Delta P_{cont}\right)}{\log(1+r)} \tag{6}$$

Given that $D_{cont} = D_l \big/ CF$, rearranging (6) to translate key parameters to normal conditions gives

$$n_{cont,new} = \frac{\log C - \log\left(D_l + \dfrac{\Delta P_{cont}}{CF}\right)}{\log(1+r)} \tag{7}$$

By comparing (3) and (7), it is noted that only when the incremental contingency power flow translated back to the normal case is the same as the incremental power flow under the normal condition, i.e. when ΔP equals to $\Delta P_{cont} \big/ CF$, the new investment horizons under the normal and contingent conditions are the same.

IV. Comparison of New Horizons for Three Test Networks

In order to investigate the difference between the two new horizons derived under normal and contingent conditions for different types of networks, an extensive comparison is carried out on three typical network configurations: single circuit, parallel circuits and meshed networks.

A. Demand Supported by Single Component

In this case, the supply to the demand will be interrupted when its supporting circuit fails, indicating that it can not be secured against N-1 contingency and consequently leading to a contingency factor of 1 for the circuit. A new connectee will only change the circuit's flow under normal situations and therefore its reinforcement is decided by the normal condition.

B. Demand Supported by Parallel Components

For a load supported by two identical parallel circuits as depicted in Fig.1, their new reinforcement horizons from the two conditions are the same if DC load flow is used and the loss along the circuits are ignored. The reason behind is that the contingent case flow increment along a circuit is twice of its normal case increment and its contingency factors is calculated as 2. In practice, however, the parallel components might not be necessarily identical and even if they are identical, their contingency factors might not be identical if the power loss along them is not neglected. Thus, their new horizons from the two cases would differ from each other; the magnitude of the difference is decided by their normal and contingent case loading conditions and contingency factors.

C. Demand Supported by Meshed Networks

The situation becomes complex for the case that demand is supplied by a meshed network. Take the system in Fig.2 as an example, in which the three circuits and the two loads are assumed to be the same, and L3 is normally open but closed in contingencies. For demonstration purposes, only L1's new horizons due to an injection at busbar 2 are analyzed. They can be calculated by submitting the power increments along it due to an injection at bus 2 under both conditions into (3) and (7), who show that bigger flow changes lead to smaller horizons.

.

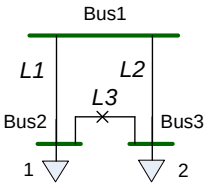

Fig. 2. Three-busbar meshed system framework.

Under normal conditions, L1's reinforcement is only triggered by the load growth at bus 2. In the contingency event that L2 fails, its future reinforcement is driven by the demand growth at both busbars 2 and 3.

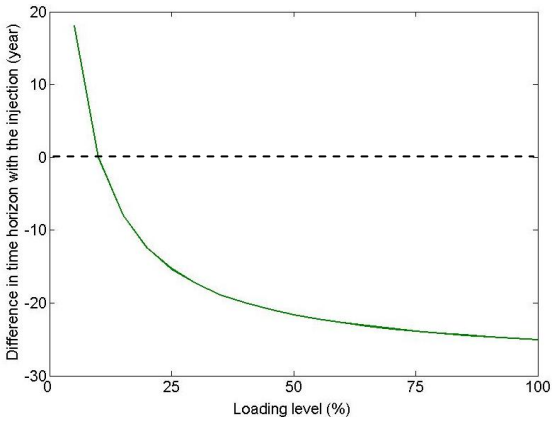

Fig. 3. Difference in L1's reinforcement horizon.

Fig.3 depicts the change of difference in L1's two new reinforcement horizons with respect to the rise of its loading level. When it is lightly loaded, the normal case horizon is bigger than the contingent case one and the difference decreases with the increasing loading level. It means that L1's future reinforcement is driven by contingent situations under lightly loaded conditions. With the rise in its loading level, a cross point is reached at a loading level of approximately 15% and beyond it the contingency driven horizon becomes bigger. It indicates that at higher loading levels, L1's reinforcement is triggered by normal situations.

One particular case needs to be pointed out when calculating L3's horizon with unequal D1 and D2. If D2 is bigger than D1, the direction of the normal case flow along L3 is from busbar 2 to busbar 3 and an injection at busbar 2 could decrease the flow. But, the injection at busbar 2 has no impact on L3 at all when L2 fails (this is the contingency event that drives L3's reinforcement). Hence, L3's contingent case horizon due to connectees at busbar 2 is always smaller than the normal case one. This point cannot be properly recognized by the original model, as it only investigates the impact in normal cases, in which the injection at busbar 2 decreases L3's normal case flow and consequently defers its reinforcement.

Components' normal and contingent reinforcement horizons would dramatically differ for meshed networks. By differentiating connectees' impact in both conditions, the proposed concept is able to better reflect the cost to the network and hence improves pricing signals in EHV distribution networks, where a large number of meshed networks exist.

V. Improved LRIC Charging Model And Sensitivity Analysis

A. Charging Model Framework

By taking components' reinforcement horizons under both normal and contingent situations into consideration and choosing the smaller ones as their actual horizons, an improved charging model is proposed, whose main procedures are outlined below:

1) Original reinforcement horizon calculation: base case flow analysis is executed to determine components' base status without any injections. The results are then fed into either (2) or (5) as they generate the same results.

2) New reinforcement horizon calculation: incremental normal case flow analysis under both normal and contingent cases is utilized to calculate flow changes along all components due to small injections. Components' new normal case horizons are determined with (3) and their new contingent case horizons are calculated with (7). For each component, the injections' impact in contingencies is assessed in the most serious contingent events that drivers their future investment. The smaller one between (3) or (7) is chosen as the new horizon.

3) Unit price calculation: once the components' old and new horizons are indentified, they are fed into the following steps to work out unit price [11].

The present value of future reinforcement of a component is

$$PV = \frac{Cost}{(1+d)^n} \tag{8}$$

where, d is the chosen discount rate and n is the component's investment horizon.

The change in present value as a result of a nodal increment for the component is

$$\Delta PV = Cost \cdot \left(\frac{1}{(1+d)^{n_{new}}} - \frac{1}{(1+d)^n} \right) \tag{9}$$

where, n and n_{new} are the component's old and new reinforcement horizons without and with an injection.

The incremental cost of the component is the annuitized change in its present value of future investment

$$\Delta IC = \Delta PV \cdot AnnuityFactor \tag{10}$$

The nodal incremental price for a studied node is the accumulation of the present value of incremental costs of all affected components supporting the node

$$LRIC = \frac{\sum \Delta IC}{\Delta PI} \tag{11}$$

where, ΔPI is the injection at the node.

B. Sensitivity Analysis to Determine Injections' Impact on Circuit Flows

As seen from part A, a large number runs of incremental normal and contingent flows need to be executed to determine the impact from injections. This could be immensely time-consuming for large-scale systems. We implemented the original and the enhanced LRIC models on a practical network with Newton power flow. The system has 1,898 busbars, 1,406 circuits, 1,044 transformers, 32 generators and a list of 675 contingencies. It takes approximately 30 minutes to evaluate nodal impact from every single node of the system and calculate nodal charges. For the enhanced model, it takes 1,670 minutes. (In the algorithm, we initialized each contingency analysis with the base case power flow results to speed up the calculation, as each contingency would only affect quite small proportion of components and most of them keep intact.). Clearly, the computational expense increases exponentially with increasing number of busbar and contingency. To reduce the computational effort, an alternative approach is to employ sensitivity analysis to determine how a tiny injection would change components' flows under both conditions [18-19]. The following analysis uses the active flow change along a component due to an injection as an example.

The active power flow along a circuit from bus i to bus j is represented by

$$P_{ij} = V_i^2 G_{ij} - V_i V_j (G_{ij} \cos\theta_{ij} + B_{ij} \sin\theta_{ij}) \tag{12}$$

If a small injection PI_n connects to node n, its effect on P_{ij} is obtained by taking derivate of (12) with respect to it

$$\frac{\partial P_{ij}}{\partial PI_n} = \frac{\partial P_{ij}}{\partial V_i}\frac{\partial V_i}{\partial PI_n} + \frac{\partial P_{ij}}{\partial V_j}\frac{\partial V_j}{\partial PI_n} + \frac{\partial P_{ij}}{\partial \theta_i}\frac{\partial \theta_i}{\partial PI_n} + \frac{\partial P_{ij}}{\partial \theta_j}\frac{\partial \theta_j}{\partial PI_n} \tag{13}$$

where, $\frac{\partial P_{ij}}{\partial V_i}$, $\frac{\partial P_{ij}}{\partial V_i}$, $\frac{\partial P_{ij}}{\partial \theta_i}$, and $\frac{\partial P_{ij}}{\partial \theta_j}$ can be calculated from (12) by calculating its partial derivatives with regard to V_i, V_j, θ_i, θ_j.

The remaining parts in (13) can be derived from the Jacobian matrix from the last iteration of power flow analysis [18].

Sensitivity analysis in normal conditions is executed based on the base case power flow analysis and, similarly, in contingencies, it is carried out based on contingency analysis of each selected contingency event.

VI. Three-busbar System Demonstration

A. Charge Calculation

In this section, the enhanced model is demonstrated and compared with the original model in [12] on the network given in Fig. 2. To simplify analysis, the three circuits are assumed to be identical, each with the rated capacity of 45 MW and cost of £1,596,700. The demand D1 and D2 are chosen as 10 MW and 20MW respectively, both of which have a growth rate of 2.0%. The injection is assumed to be 1 MW.

The calculated results with and without an injection at busbars 2 and 3 are provided in Table I. As seen, although the three circuits are identical, their contingency factors and maximum available capacity vary dramatically. L2 has the smallest contingency factor, 1.8, leading to the maximum available capacity of 25MW. L3's contingency factor is the biggest, 6.0 and it scales its maximum available capacity down to merely 7.5MW. Bigger contingency factors mean that the circuits need to carry larger volume of contingency flows, which in turn lead to small capacity available under normal conditions.

Table I
Results of the three–busbar system

Circuit No.	L1	L2	L3
Normal flow (MW)	13.33	16.67	3.33
Maximum contingency flow (MW)	30	30	20
Most serious contingency	L2 out	L1 out	L2 out
Contingency factor	2.25	1.80	6.0
Maximum available capacity (MW)	20	25	7.5
$\Delta P_{cont}/CF$ (injection at bus 2) MW)	0.44	0.56	0.0
ΔP (injection at bus 2) (MW)	0.67	0.33	-0.33
$\Delta P_{cont}/CF$ (injection at bus 3) (MW)	0.44	0.56	0.17
ΔP (injection at bus 3) (MW)	0.33	0.67	0.33

When an injection connects to either bus 2 or bus 3, all circuits' maximum contingency flow increments are 1MW in their most contingencies. For example, when L2 fails, the injection at busbar 2 will increase both L1's and L3's contingency flow by 1MW. $\Delta P_{cont}/CF$ becomes to 0.44MW, 0.56MW and 0.0MW respectively for the three circuits. In normal conditions, however, an injection at busbar 2 causes the three circuits' normal flow to change, ΔP, by 0.67MW, 0.33MW and -0.33MW respectively. The negative increment means that the injection can reduce L3's normal case flow. By comparison the two cases, the injection has greater impact on L1 in normal conditions, which is exactly reverse for L2. As regard to L3, the power increment has no impact on it in contingencies, whereas it brings down its flow in normal conditions. To further elaborate the difference, the circuits' reinforcement horizons are provided in Table II.

Table II
Reinforcement horizons in the two conditions (yr)

Circuit No.		L1	L2	L3
No injection	Nor. case	40.75	40.75	81.50
	Con. case	40.75	40.75	81.50
Injection at Bus 2	Nor. case	35.85	38.76	92.09
	Con. case	37.45	37.45	81.50
Injection at Bus 3	Nor. case	38.27	36.81	71.92
	Con. case	37.45	37.45	76.59

Note: "nor." stands for "normal" and "con." stands for" contingency".

As expected, the two approaches produce the same results when no injections are connected, whereas with new injections, the circuits' reinforcement horizons from the two cases differ. One point should be noted is that when an injection connects to busbar 2, L3's contingency horizon is equal to its original horizon, 81.50yrs, smaller than the normal horizon of 92.09yrs. It means that the injection does not affect L3 in contingencies but defers its horizon in normal conditions. If the smaller horizon is deemed as the true timing for investment, L3's reinforcement therefore is driven by contingent case. The original model is not able to identify this case as it examines the impact only in normal conditions.

The incremental costs from each circuit and the total nodal charges for the two load busbars evaluated with the horizons in Table II are outlined in Table III.

Table III
Results for the three-busbar system (£/MW/yr)

		Cost from L1	Cost from L2	Cost from L3	Total charge
Improved model	Bus 2	3019.87	1918.78	0.00	4938.66
	Bus 3	1918.78	2347.17	460.42	4726.37
Original model	Bus 2	3019.87	1108.01	-260.69	3867.19
	Bus 3	1405.06	2347.17	460.42	4212.65

For both approaches, a large proportion of the charge at busbar 2 is from the incremental cost of L1, and at busbar 3, it mainly comes from L2's cost, as injections at the two buses greatly increase their loading levels in both situations. One interesting point is that the incremental cost from L3 for busbar 2 is zero in the improved approach, as an injection at busbar 2 does not change L3's reinforcement horizon. The original model, however, produces a cost of -260.69 £/MW/yr busbar 2. Although an injection at busbar 2 can bring down L3's normal case horizon, it has no impact on L3 in the contingency that drives its reinforcement.

The enhanced model produces bigger costs from all three circuits and consequently the bigger final total charges for the two busbars compared with original model. The ultimate nodal charges are 4938.66 £/MW/yr at bus 2 and 4726.37 £/MW/yr at bus 3 from the new model, higher than 3867.19 £/MW/yr and 4212.65 £/MW/yr from the original model respectively.

B. The Impact of Different Influencing Factors

The impact of three major factors that affect final charges -,

loading level, load growth and nodal injection size- on the charge difference is examined in this part. For simplicity, the load at busbar 3 is assumed to be 2 times of that at busbar 2 and only the charge at busbar 1 is investigated.

Fig.4 shows that with the increase of system loading conditions, the charge difference widens gradually. When the load amount at busbar 1 is over 11MW, the difference grows bigger than 1837.63 £/MW/yr, which becomes even large with the rise in loading level. The reason behind is that higher loading levels produce nearer reinforcement horizons, hence leading to higher charges and consequently greater difference.

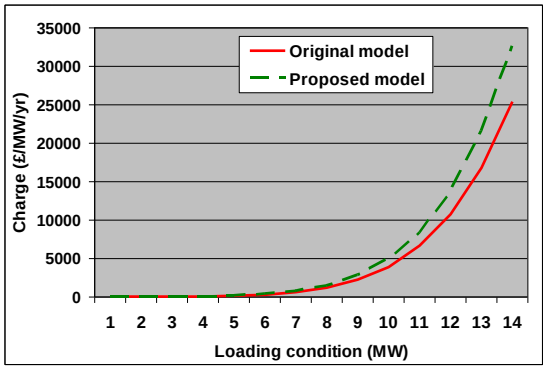

Fig. 4. Charge comparison under different loading levels.

Fig.5 demonstrates the change in the difference with respect to the rise of load growth rate. It is relatively small when the rate is smaller than about 0.4%, but grows steadily when it is over 1%. One important point is that when load growth rate is approximately 1.6%, the charges from the original model decrease after a summit is reached. It is because the load at busbar 2 would have even greater negative cost, i.e. reward, for using L3 beyond that rate. By contrast, the proposed model produces consistent increasing charges with the rise of load growth rate, as no costs from the three circuits are negative.

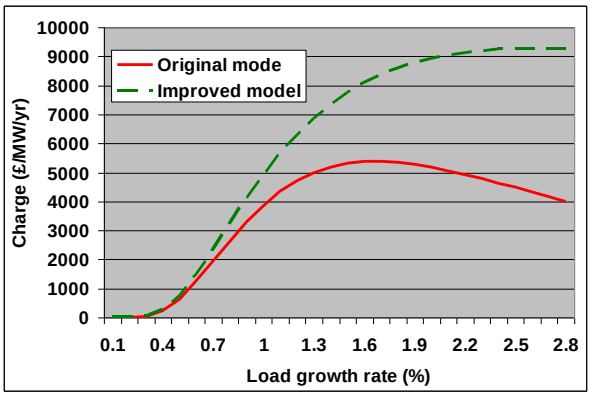

Fig. 5. Charge comparison under different load growth rates.

With regard to the injection size, it influences the charge difference slightly as demonstrated in Fig.6. When it is small, the difference tends to be small, which grows slowly when the injection grows bigger.

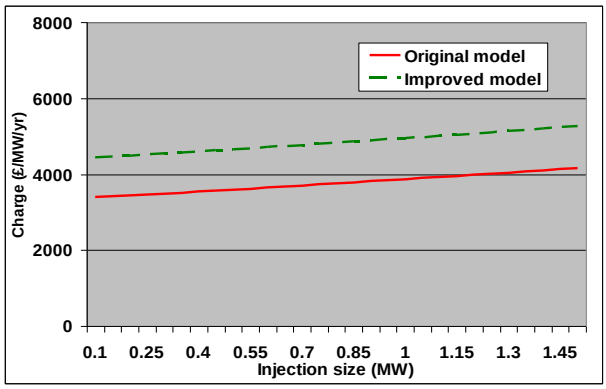

Fig. 6. Charge comparison under different injection size.

VII. Demonstration on a Practical System

In this section, the comparison of the two approaches is carried out on a practical Grid Supply Point (GSP) area taken from the U.K. distribution network, given in Fig.9. The load growth rate and injection size are chosen as 2.0% and 0.01MW respectively. Security standard is set as N-1 contingencies. The circuit linking busbar 1005 and 1007 is not considered in this study as it is owned by the generator at busbar 1002 rather than the local DNO.

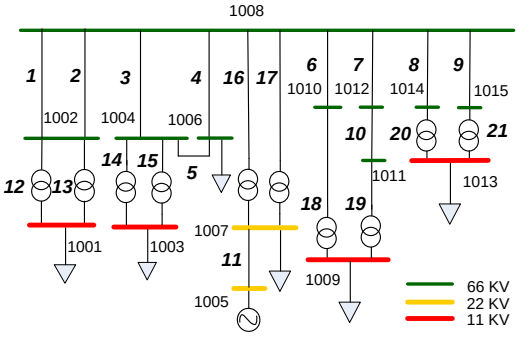

Fig.7. A GSP area test system.

Table IV
Contingency factors and maximum available capacity of all components

No.	Contingency factor	Maximum available capacity (MVA)	No.	Contingency factor	Maximum available capacity (MVA)
L1	1.99	24.95	L12	2.05	14.04
L2	2.01	24.71	L13	2.05	14.04
L3	2.05	26.77	L14	2.04	19.59
L4	1.98	27.66	L15	2.07	19.33
L5	3.77	16.21	L16	1.95	16.06
L6	2.04	17.95	L17	2.12	14.76
L7	1.93	12.32	L18	2.00	19.97
L8	2.05	9.31	L19	2.04	19.65
L9	2.05	9.30	L20	2.02	14.21
L10	2.07	17.49	L21	2.03	14.19

All components' contingency factors and their maximum available capacity from the original model are given in Table IV. As noticed, the contingency factors for those parallel components are not necessarily 2 as they are not exactly identical, and in addition, they are also influenced by the power loss along them. Circuit No.5 has the biggest

contingency factor of 3.77, which reduces its maximum available capacity from 61.16MVA down to merely 16.21MVA. The maximum available capacity of all other branches is also brought down in proportion to their contingency factors.

To assist the analysis, Fig. 8 provides all branches' utilization levels. The most heavily loaded circuit is L2 linking buses 1004 and 1006, and by contrast, L3 has the smallest loading level, merely approximately 14%. These loading conditions are calculated on the base of branches' rated capacity and they might be even higher if calculated on the basis of their maximum available capacity.

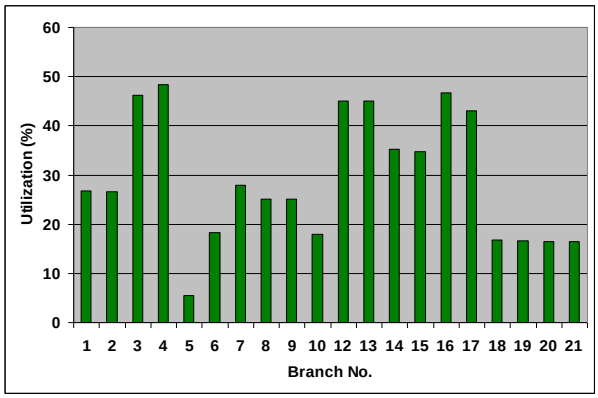

Fig.8. Base case circuit utilization levels.

Table V outlines the active power changes along all branches in normal conditions and the changes in their most serious contingency events over their contingency factors (hereafter referred as contingent flow change for simplicity).

TABLE V
COMPARISON OF ACTIVE POWER FLOW CHANGE IN THE TWO CONDITIONS (10^{-3}/MW)

1001	No.	L1	L2	L12	L13	
	Nor.	5.0854	5.0332	5.0260	5.0261	
	Con.	5.0847	5.0377	4.9353	4.9355	
1003	No.	L3	L4	L5	L14	L15
	Nor.	5.1206	5.0648	5.0345	5.0624	4.9988
	Con.	5.0077	5.1724	2.6852	4.9620	4.8961
1006	No.	L3	L4	L5		
	Nor.	4.7548	5.2983	-4.7285		
	Con.	4.9403	5.0951	0.0000		
1007	No.	L16	L17			
	Nor.	5.2271	4.8116			
	Con.	5.1856	4.7644			
1009	No.	L6	L7	L10	L18	L19
	Nor.	5.0390	5.0062	4.9926	5.0242	4.9865
	Con.	4.9530	5.2393	4.8583	5.0059	4.9267
1013	No.	L8	L9	L20	L21	
	Nor.	5.0185	5.0098	5.0087	5.0000	
	Con.	4.9138	4.9049	4.9562	4.9473	

When an injection is connected to busbar 1001, its three supporting branches, L1, L13 and L14 have bigger normal case flow changes than the contingent ones. One exception is L2, which has a bigger contingency flow change increment, counted as 5.0377×10^{-3}MW. An injection at busbar 1003 can cause greater normal case flow changes for its supporting branches, L3, L5, L14, and L15. For example, L5's normal flow change is 5.0345×10^{-3}MW, which is almost 2 times of the contingency flow change, 2.6852×10^{-3}MW. The reason is that although L5's biggest extra contingency flow change is approximately 0.01MW when L3 fails, it has a bigger contingency factor, 3.77, which greatly scales down the contingency flow change. It should be noted that an injection at busbar 1006 reduces L5's normal flow by -4.7285×10^{-3}MW, but it does not affect it in contingencies. Bigger extra power flows bring components' reinforcement horizons closer, zero extra flows cause no impact at all, and negative extra flows defer the horizons. The bigger flows in contingencies indicate that they drive the reinforcement of components.

The flow changes along a branch due to nodal injections are decided by several factors in both conditions, such as system topologies, component parameters, loading levels, contingency types, and injections sizes, etc. More complex networks could produce diversified results. For instance, a load that withdraws power at a busbar located far from power sources would have greater impact on the components closer to the sources as the power losses along all supporting branches accumulate gradually. To demonstrate this point, a part is taken from the 1,898-busbar system, as shown in Fig.9.

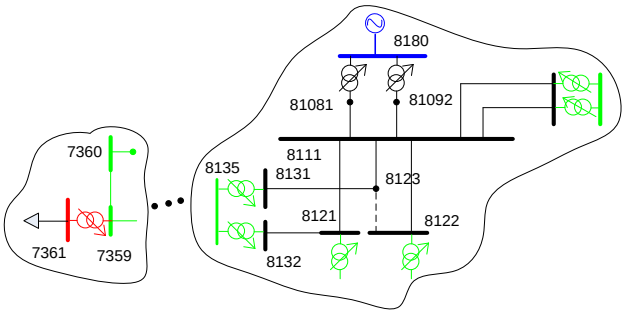

Fig.9. A part of EHV distribution network.

The contingency factor of the 132KV circuit 8111-8123 is 1.69 and its reinforcement is driven by the outage of busbar 8121. When a nodal injection of 0.1MW comes to busbar 7361, which is far from the circuit but supported by it, its normal case flow change is 0.038 MW. When busbar 8121 fails, the flow change is 0.079MW, becoming to 0.047MW if divided by its contingency factor. The flow difference is 0.009MW. Therefore, the nodal injection at busbar 7361 drives the circuit 8111-8123 reinforcement in contingencies.

As proposed, it is easier and time-saving to carry out sensitivity analysis to determine injections' impact, which would not jeopardize accuracy. For the same large 1,898-busbar system, the total computational time is reduced to 3 minutes to determine the injections' impact in normal conditions and 209 minutes in contingencies. The total running time is reduced to nearly 1/10 of the simulation approach; the time saving is enormous.

The sensitivity coefficients from both normal and contingent situations reflecting how a unit injection at each studied busbar affects components' flows in the two conditions are given in Table VI.

TABLE VI
SENSITIVITY ANALYSIS UNDER THE TWO CONDITIONS (10^{-3}/MW)

1001	No.	L1	L2	L12	L13	
	Nor.	5.085	5.033	5.025	5.025	
	Con.	5.084	5.038	4.938	4.938	
1003	No.	L3	L4	L5	L14	L15
	Nor.	5.121	5.065	5.035	5.062	4.999
	Con.	5.010	5.172	2.685	4.967	4.900
1006	No.	L3	L4	L5		
	Nor.	4.755	5.298	-4.728		
	Con.	4.941	5.095	0.000		
1007	No.	L16	L17			
	Nor.	5.226	4.810	-		
	Con.	5.186	4.764	-		
1009	No.	L6	L7	L10	L18	L19
	Nor.	5.039	5.006	4.993	5.024	4.986
	Con.	4.953	5.239	4.858	5.005	4.926
1013	No.	L8	L9	L20	L21	
	Nor.	5.019	5.010	5.008	4.999	
	Con.	4.914	4.905	4.956	4.947	

By comparing with the simulation approach, sensitivity analysis produces quite close results. For example, the sensitivities at busbar 1003 also indicate that an injection at this bus has greater impact on L1, L13 and L14 in normal conditions, but less on L2 in normal cases. The contingent case sensitivity for L5 with demand increase at busbar 1003 is 2.685×10^{-3}MW and the normal case one is 5.035×10^{-3}MW, showing the same pattern as given in Table V. Further, the impact from an injection at busbar 1006 on L5 can also be captured by the sensitivities: it reduces L5's normal flow, but has no impact on it in contingencies. Although sensitivity analysis cannot provide results as precise as simulation approach, it is capable to produce very close results especially when injections are small.

TABLE VII
COMPONENTS' NEW HORIZONS FROM THE TWO CONDTIONS (YR)

1001	No.	L1	L2	L12	L13	
	Nor.	34.7316	34.7036	6.9729	6.9697	
	Con.	34.7317	34.7035	6.9733	6.9701	
1003	No.	L3	L4	L5	L14	L15
	Nor.	7.3565	7.3818	34.4117	12.7984	12.7535
	Con.	7.3567	7.3816	34.4262	12.7987	12.7539
1006	No.	L3	L4	L5		
	Nor.	7.3573	7.3813	34.4719		
	Con.	7.3569	7.3818	34.4427		
1007	No.	L16	L17			
	Nor.	7.8986	7.7886			
	Con.	7.8988	7.7888			
1009	No.	L6	L7	L10	L18	L19
	Nor.	52.8960	33.5071	53.0635	57.8360	57.8374
	Con.	52.8967	33.5053	53.0646	57.8361	57.8379
1013	No.	L8	L9	L20	L21	
	Nor.	36.5565	36.5513	58.5115	58.5087	
	Con.	36.5577	36.5525	58.5121	58.5093	

By using the flow changes in Tables V or VI, all components' new reinforcement horizons under the two conditions are derived, given in Table VII. Although for most cases they are rather close, the horizons still differ for some components, which eventually generate great difference in nodal charges.

The finally calculated charges from the original and improved models are together outlined in Table VIII.

TABLE VIII
CHARGES OBTAINED USING THE TWO METHODS (£/KW/YR)

Busbar No.	1001	1003	1006	1007	1009	1013
Original method	6.372	18.860	15.515	2.461	8.938	6.638
Improved method	6.373	19.013	16.559	2.461	9.256	6.638

As observed, the charges from the enhanced approach are always not smaller than those from the original model. Busbars 1001, 1007 and 1013 are supported by two groups of similar parallel branches respectively and the two approaches produce nearly the same charges. For busbar 1009 supported by non-similar parallel components, its charge difference grows to 0.318 £/kW/yr. Busbars 1003 and 1006, supported by meshed networks, witness even great charge difference: 0.157 £/kW/yr and 1.04 £/kW/yr respectively. Although the charge difference is not significant here, it can grow large for large-scale and highly meshed EHV distribution networks.

For the partial system in Fig.9, the cost of the circuit 811-8123 is £2.4 million. The incremental cost from the original LRIC is 10.47 £/kW/yr for customers at busbar 7361, which becomes to 12.90 £/kW/yr from the enhanced model, giving a difference of 2.43 £/kW/yr. For a distributed generation with a capacity of 60MW, the difference in use of system charges per year would be £146k per year. This large difference indicates the importance of considering customers' impact in contingencies on network components in network pricing.

VIII. CONCLUSION

This paper improves the existing LRIC model by considering the impact of a nodal injection on network components under both normal and contingent conditions. Sensitivity analysis is introduced here to substantially reduce calculation burden. Based on the intensive study on two examples, the following key observations are reached:

1) In terms of reflectivity, the original LRIC charging model reflects network security with contingency factors to shape components' maximum available capacity and then determine how they would affect components only in normal conditions. The proposed approach, by expanding the scope of the original model, can recognize the impact in both normal and contingent situations, being able to actually reflect users' use of system.
2) In term of difference, the proposed method chooses the smaller new horizons from the two conditions to calculate nodal charges. Thus, the charges from it are always not smaller than those from the original model. The difference varies dramatically, depending on loading levels, load growth rates, and injection sizes as well as network topology.
3) In terms of simplicity, the original model needs one run power flow analysis, one full contingency analysis, and *N*

(the number of studied busbars) runs of incremental power flow analysis to assess injections' impact. Apart from these calculations, the proposed approach needs to run full incremental contingency analysis to determine injections' impact in contingencies.

The major contributions of this paper are:

1) It developed an enhanced LRIC model that respects the differences in the impacts to the network from network users under both normal and contingent conditions.
2) It mathematically identifies the conditions when the impacts under the two conditions conform and when they differ, and which condition drives reinforcement. It respects how nodal injections affect components' reinforcement in meshed networks under both conditions and thus generates charges/rewards accordingly, which is not properly handled by the original model.
3) It developed sensitivity analysis to reduce the significant rise in computational burden as a result of increasing simulating nodal injections under contingencies. The developed approach can approximate the extent to which a nodal injection would affect components under both situations, reducing computational expenses by nearly 90% and making it practical for large practical networks

IX. Appendix

Most Serious Contingency: it is the contingency event for a component that leads to its largest flow under such event. The most serious contingency for different network components could be differing;

Maximum Contingency Flow: it is the flow along a particular component under its most serious contingency;

Contingency Factor: it is calculated by dividing the maximum contingency flow along a component with its normal case flow.

Maximum Available Capacity: it is calculated by diving a component's rated capacity with its contingency factor. The future demand and generation can only increase within the threshold of this value of their supporting components.

X. References

[1] D. Shirmohammadi, *et al.*, "Some fundamental, technical concepts about cost based transmission pricing," *Power Systems, IEEE Transactions on*, vol. 11, pp. 1002-1008, 1996.

[2] Z. Jing, *et al.*, "Review of transmission fixed costs allocation methods," in *Power Engineering Society General Meeting, 2003, IEEE*, 2003, pp. 2585-2592.

[3] J. Pan, *et al.*, "Review of usage-based transmission cost allocation methods under open access," *Power Systems, IEEE Transactions on*, vol. 15, pp. 1218-1224, 2000.

[4] J. W. Marangon Lima, "Allocation of transmission fixed charges: an overview," *Power Systems, IEEE Transactions on*, vol. 11, pp. 1409-1418, 1996.

[5] P. M. Sotkiewicz and J. M. Vignolo, "Allocation of fixed costs in distribution networks with distributed generation," *Power Systems, IEEE Transactions on*, vol. 21, pp. 639-652, 2006.

[6] H. H. Happ, "Cost of wheeling methodologies," *Power Systems, IEEE Transactions on*, vol. 9, pp. 147-156, 1994.

[7] R. R. Kovacs and A. L. Leverett, "A load flow based method for calculating embedded, incremental and marginal cost of transmission capacity," *Power Systems, IEEE Transactions on*, vol. 9, pp. 272-278, 1994.

[8] M. T. Ponce de Leao and J. T. Saraiva, "Solving the revenue reconciliation problem of distribution network providers using long-term marginal prices," *Power Systems, IEEE Transactions on*, vol. 18, pp. 339-345, 2003.

[9] J. W. Marangon Lima and E. J. de Oliverira, "The long-term impact of transmission pricing," *Power Systems, IEEE Transactions on*, vol. 13, pp. 1514-1520, 1998.

[10] D. Shirmohammadi, *et al.*, "Cost of transmission transactions: an introduction," *Power Systems, IEEE Transactions on*, vol. 6, pp. 1546-1560, 1991.

[11] F. Li and D. L. Tolley, "Long-Run Incremental Cost Pricing Based on Unused Capacity," *Power Systems, IEEE Transactions on*, vol. 22, pp. 1683-1689, 2007.

[12] H. Y. Heng, *et al.*, "Charging for Network Security Based on Long-Run Incremental Cost Pricing," *Power Systems, IEEE Transactions on*, vol. 24, pp. 1686-1693, 2009.

[13] Frontier. (2008). *Review of distribution use of system charging methodology*. Available: http://www.eon-uk.com/downloads/FrontierEconomicsG3DUoSChargesFinal250308.pdf

[14] F. Li, "The Benefit of a Long-run Incremental Pricing Methodology to Future Network Development," in *Power Engineering Society General Meeting, 2007. IEEE*, 2007, pp. 1-2.

[15] F. Li, "Recent developments in common distribution network pricing in Great Britain," in *Energy Market (EEM), 2010 7th International Conference on the European*, 2010, pp. 1-5.

[16] F. Li, "Recent developments in common distribution network pricing in Great Britain," in *Energy Market (EEM), 2010 7th International Conference on the European*, 2010, pp. 1-5.

[17] W. A. (2010). *FCP methodology implementation and guidance notes*. Available: http://2010.energynetworks.org/

[18] C. Gu and F. Li, "Long-Run Marginal Cost Pricing Based on Analytical Method for Revenue Reconciliation," *Power Systems, IEEE Transactions on*, vol. 26, pp. 103-110, 2011.

[19] C. Gu and F. Li, "Sensitivity analysis of long-run incremental charge based on analytical approach," in *Electricity Distribution - Part 1, 2009. CIRED 2009. 20th International Conference and Exhibition on*, 2009, pp. 1-4.

Chenghong Gu (S'09) was born in Anhui province, China. He received his, Bachelor degree and Master degree in electrical engineering from Shanghai University of Electric Power and Shanghai Jiao Tong University, Shanghai, China, in 2003 and 2007 respectively. In 2010, he obtained his PhD from University of Bath, U.K. Now, he is working as a KTA fellow in the Dept. of Electronic & Electrical Eng., University of Bath. His major research is in the area of power system economics and planning.

Furong Li (M'00, SM'09) was born in Shannxi province, China. She received the B.Eng. degree in electrical engineering from Hohai University, Nanjing, China, in 1990 and the Ph.D. degree from Liverpool John Moores University, Liverpool, U.K., in 1997. She then took up a lectureship with Department of Electronic & Electrical Engineering, University of Bath, where she is a Reader in the Power and Energy Systems Group at the University of Bath, Bath, U.K. Her major research interest is in the area of power system planning, analysis, and power system economics.